Environment International 73 (2014) 346–358

Contents lists available at ScienceDirect

Environment International

journal homepage: www.elsevier.com/locate/envint

Wildfires in Chernobyl-contaminated forests and risks to the population and the environment: A new nuclear disaster about to happen?

Nikolaos Evangeliou [a,*], Yves Balkanski [a], Anne Cozic [a], Wei Min Hao [b], Anders Pape Møller [c]

[a] Laboratoire des Sciences du Climat et de l'Environnement (LSCE), CEA–UVSQ–CNRS UMR 8212, Institut Pierre et Simon Laplace, L'Orme des Merisiers, F-91191 Gif-sur-Yvette Cedex, France
[b] Missoula Fire Sciences Laboratory, Rocky Mountain Research Station, United States Forest Service, Missoula, MT, USA
[c] Laboratoire d'Ecologie, Systématique et Evolution, CNRS UMR 8079, Université Paris-Sud, Bâtiment 362, F-91405 Orsay Cedex, France

ARTICLE INFO

Article history:
Received 23 June 2014
Accepted 20 August 2014
Available online xxxx

Keywords:
Chernobyl accident
Forest fires
Redistribution
Radionuclides
Risks

ABSTRACT

Radioactive contamination in Ukraine, Belarus and Russia after the Chernobyl accident left large rural and forest areas to their own fate. Forest succession in conjunction with lack of forest management started gradually transforming the landscape. During the last 28 years dead wood and litter have dramatically accumulated in these areas, whereas climate change has increased temperature and favored drought. The present situation in these forests suggests an increased risk of wildfires, especially after the pronounced forest fires of 2010, which remobilized Chernobyl-deposited radioactive materials transporting them thousand kilometers far. For the aforementioned reasons, we study the consequences of different forest fires on the redistribution of ^{137}Cs. Using the time frequency of the fires that occurred in the area during 2010, we study three scenarios assuming that 10%, 50% and 100% of the area are burnt. We aim to sensitize the scientific community and the European authorities for the foreseen risks from radioactivity redistribution over Europe. The global model LMDZORINCA that reads deposition density of radionuclides and burnt area from satellites was used, whereas risks for the human and animal population were calculated using the Linear No-Threshold (LNT) model and the computerized software ERICA Tool, respectively. Depending on the scenario, whereas between 20 and 240 humans may suffer from solid cancers, of which 10–170 may be fatal. ERICA predicts insignificant changes in animal populations from the fires, whereas the already extreme radioactivity background plays a major role in their living quality. The resulting releases of ^{137}Cs after hypothetical wildfires in Chernobyl's forests are classified as high in the International Nuclear Events Scale (INES). The estimated cancer incidents and fatalities are expected to be comparable to those predicted for Fukushima. This is attributed to the fact that the distribution of radioactive fallout after the wildfires occurred to the intensely populated Western Europe, whereas after Fukushima it occurred towards the Pacific Ocean. The situation will be exacerbated near the forests not only due to the expected redistribution of refractory radionuclides (also trapped there), but also due to the nutritional habits of the local human and animal population.

1. Introduction

The accident in Chernobyl Nuclear Power Plant (CNPP) in 1986 resulted in the release of over 10 EBq ($\times 10^{18}$ Bq) of fission and activation products from the damaged Reactor 4 (De Cort et al., 1998). Around 2 EBq – the most refractory (^{144}Ce, ^{141}Ce, ^{106}Ru, ^{140}Ba, ^{95}Zr, ^{99}Mo, $^{238–241}$Pu, ^{241}Am etc.) – was deposited in the 30 km vicinity of the power plant (Hatano et al., 1998) known as the Chernobyl Exclusion Zone (CEZ, 25°–31°E and 48°–52°N), between 29°–31°E and 52°–54°N (Gomel, Belarus) and between 33°–40°E and 52°–54°N (Russia) (De Cort et al., 1998). The rest (^{137}Cs, ^{90}Sr, ^{134}Cs, ^{131}I and noble gases) flew and fell over the rest of the world according to the prevailing meteorological conditions.

Since then, the landscape in these areas has changed. Gradually, as no one was able to cut saplings and cultivate fields anymore, natural ecological succession began transforming these regions. The forests that covered 53% of the area before the disaster cover more than 70% 15 years later (IAEA, 2001). Stands dominated by Scots pine have taken over pastures, where farmers used to grow wheat and flax, and open patches (studded with young pines and birches) have overwhelmed the areas. Nowadays radionuclides have migrated into the forest soil and basically stayed there. It has been reported that 90% of ^{90}Sr has been found in the top 10 cm of the soil in the Red Forest (IRL, 2013), whereas around 80% of ^{137}Cs is in the top 5 cm in the adjacent areas (Yablokov et al., 2009). Trees, grasses, other plants, and fungi trap radionuclides during their basic life cycle. During transpiration (release water), the plant draws more water up from the roots.

* Corresponding author at: Laboratoire des Sciences du Climat et de l'Environnement (LSCE), CEA–CNRS–UVSQ, Institut Pierre et Simon Laplace, L'Orme des Merisiers, F-91191 Gif sur Yvette Cedex, France. Tel.: +33 1 6908 1278; fax: +33 1 6908 3073.
E-mail address: Nikolaos.Evangeliou@lsce.ipsl.fr (N. Evangeliou).

http://dx.doi.org/10.1016/j.envint.2014.08.012
0160-4120/

Conservative salts of cesium and strontium, which are chemical analogs of potassium and calcium, respectively, substitute these crucial nutrients. The needles then fall to the ground, becoming part of the "litter" (the vegetation that covers the forest floor) and returning radioactive salts to the top layer of the soil. Without the trees or other permanent groundcover, contaminants would migrate away, blown in dust or carried by water.

There has hardly been any forestry activity in the CEZ and similar restricted access areas since 1986, except for clearing of areas near roads. The areas are populated by CNPP workers, police servants, as well as some locals, who refused to evacuate their houses after the disaster and live cultivating the land. Thus, there has been continuous accumulation of dead wood and other plant material since 1986. This effect of accumulation of dead plant matter is exacerbated by dramatically reduced decomposition of biological material in contaminated areas (Mousseau et al., 2014). As a result, there is an increasing frequency of fires in the region. For example, MODIS (Moderate Resolution Imaging Spectroradiometer) satellite showed 54 fires in contaminated areas in 2010 and more than 300 in other areas. Most of these fires are agricultural ones, as farmers habitually light them on their fields to burn weeds, potato stems and other plant material, and such fires can lead to uncontrolled forest fires. In addition, many fires in contaminated areas may be due to natural causes such as lightning. Climate near CNPP has become increasingly warmer in spring and summer since 1990, and precipitation has been stabilized or slightly decreased during the same period (Evangeliou et al., accepted). This was most pronounced during July–August 2010, when temperatures exceeding 40 °C accompanied many weeks without precipitation. With the projected increase in CO_2 and other greenhouse gases suggested by the Intergovernmental Panel on Climate Change models (e.g. IPCC, 2013), the occurrence of exceedingly warm and dry summers is expected to increase.

All organic materials in contaminated areas contain radioactive material, and hence any fire will disperse radionuclides in a way that will depend on surface heat flux released by the fire, prevailing wind and precipitation patterns particularly during the summer months July–August, when the risk of fire is higher. The spatial distribution of radioactivity is currently well known either from measurements (e.g. De Cort et al., 1998; Kashparov et al., 2003) or modeling (e.g. Brandt et al., 2002; Evangeliou et al., 2013a). Recent studies have shown significant migration of radionuclides from the exclusion zone towards Kiev (MUEAPPCCC, 2008). There is also considerable evidence of firewood use for cooking and heating in private houses causing considerable levels of radioactivity indoors (Dancause et al., 2010). Likewise, burning of dried potato stalks during fall increases radiation levels in fields many times higher comparing to the contamination from the original catastrophe in 1986 (Dancause et al., 2010).

This paper presents three different scenarios of forest fires: (a) minor fires that cover 10% of the forests in Ukraine, Belarus and Russia, which can be extinguished by humans, (b) intermediate fires that affect 50% of the same forests, and (c) a worst case scenario, in which the entire area is affected by fires. We study how the aforementioned forest fires (from now on 2010_scenario_10, 2010_scenario_50, 2010_scenario_100) may redistribute radioactive materials over Europe. The temporal variability of these fires has been adopted from MODIS for the fires of 2010 that were the most severe events of the last decade. More specifically, we keep the timeline of fires in these forests as in 2010 and assume that more pixels (larger surface) are burnt covering 10%, 50% and 100% of the forest area. Small fires occur on a regular basis in these areas, and the rudimentary fire extinguishing equipment available is of a magnitude that may allow termination of such fires. Intermediate fires covering 50% of the area have not happened yet, but are certainly a possibility, especially given the extensive forest fires during summer 2010. Once a fire is so large that it cannot readily be extinguished by local equipment, there is the potential for a large-scale fire that cannot even be extinguished by aerial firefighting and other large equipment. Given the socioeconomic situation in Ukraine and the crisis on the political relationships with Russia (which would be expected to provide assistance in case of an emergency), a scenario of a wildfire becomes a possibility. We study the redistribution of ^{137}Cs under these three scenarios, a radionuclide of major concern, due to its half-life (30.2 years), the radiation type it emits during its radioactive decay and its bioaccumulation by organisms (chemical analogue of potassium with high mobility in biological systems, Woodhead, 1973). Besides, it constitutes the global fallout after a major nuclear incident and is transported over long distances. We predict the public health consequences of forest fires and the consequences for animals and plants. Because the public health consequences of radioactive contamination are so disputed, we make direct estimates of the effects of forest fires on public health (using the Linear No-Threshold model) or animals and plants (using the ERICA Tool). Concerning organisms, we discuss the results of the tool in comparison with the evolutionary observations reported by Møller and Mousseau (2006), who have already quantified the relationship between species richness and abundance, respectively, and level of background radiation for radioactively contaminated areas in Ukraine, Belarus and Russia.

2. Methodology

2.1. Model characteristics, emission factor and injection heights

The aerosol module INCA (INteractions between Chemistry and Aerosols) is coupled to the general circulation model (GCM), LMDz (Laboratoire de Météorologie Dynamique), and the global vegetation model ORCHIDEE (ORganizing Carbon and Hydrology In Dynamic Ecosystems Environment) (LMDZORINCA) (Szopa et al., 2012). Aerosols and gases are treated in the same code to ensure coherence between gas phase chemistry and aerosol dynamics, as well as possible interactions between gases and aerosol particles. The standard model horizontal resolution is 2.50° in longitude and 1.27° in latitude. However, the GCM also offers the possibility to zoom over specific regions by stretching the grid with the same number of grid-boxes. In the present study the zoom version was used to simulate fires in Europe achieving a resolution of 0.45° × 0.51°. On the vertical, the model uses sigma-p coordinates with 19 levels extending from the surface up to about 3.8 hPa corresponding to a vertical resolution of about 300–500 m in the planetary boundary layer and to a resolution of about 2 km at the tropopause.

Each simulation lasted until the end of the year, which is a sufficient period for most ^{137}Cs to be deposited as seen from the Chernobyl and Fukushima accidents (Brandt et al., 2002; Paatero et al., 2012). LMDZORINCA accounts for emissions, transport (resolved and subgrid scale), photochemical transformations, and scavenging (dry deposition and washout) of chemical species and aerosols interactively in the GCM (schemes are described in detail in Evangeliou et al., 2013a). Several versions of the INCA model are currently available depending on the envisaged applications with the chemistry-climate model. The model runs in a nudged mode (using the ERA40 Re-analysis data — 6 h wind fields, ECMWF, 2002) with a relaxation time of 10 days for the regular grid, whereas for the zoom version relaxing to 4.8 days in the center of the zoom and to 10 days outside (Hourdin and Issartel, 2000). Cesium-137 was inserted as an inert tracer within the model and mostly behaves as an aerosol and as such it is treated in the model (Ritchie and McHenry, 1990; Yoschenko et al., 2006).

An important factor in our simulations was the emission factor of ^{137}Cs after a fire event, namely the fraction that will be emitted compared to what is present on the ground or in the biomass. Yoschenko et al. (2006) reported that this fraction is 4% conducting fire experiments in Chernobyl (small, controlled fires) and measuring budgets. Amiro et al. (1996) found that the emission factor ranges between 20 and 100% depending on the temperature of burning of straw, pine and aspen. Horrill et al. (1995) performed experiments for heather burning and found that 10–40% of ^{137}Cs would be emitted

after heather fires depending again on the temperature (12% after a cool burning and 39% after a hot burning). Finally, Piga (2010) performed similar fire experiments in an artificial experimental site using contaminated wood as fuel finding a redistribution of approximately 10% for ^{137}Cs. Beyond biomass, the fate of ^{137}Cs deposited in the soil and how much would escape to the atmosphere after a fire event are of major importance. Cesium-137 is accumulated in the top-soil layer (Yablokov et al., 2009) and remains there for many years (presenting small migration velocities, Lujanieneo et al., 2002). It presents a low boiling point (669 °C) and it is lost in the smoke even when located in the soil through volatilization. Paliouris et al. (1995) showed that the redistribution from soil is more than 20% in North American boreal forests.

No available measurements of radioactivity in biomass all over the contaminated forests of Ukraine, Belarus and Russia exist, except for few scattered measurements. Therefore, we assume that each pixel consists of biomass available to be burnt and that ^{137}Cs is deposited within the biomass. We expect that the assumption of the whole pixel filled by biomass is more or less accurate, as, according to Yoschenko et al. (2006), Amiro et al. (1996), Horrill et al. (1995), Piga (2010) and Paliouris et al. (1995), ^{137}Cs will be redistributed in the atmosphere no matter if it is deposited in soil, biomass or vegetation. We account for a relatively conservative emission factor of ^{137}Cs (40% of what is deposited will be re-emitted), despite that this portion may rise up to 100% (in high temperatures of a wildfire).

Injection height also appears to be a key agent that controls transport and final deposition of radioactive material redistributed from fires. The 2010 fires in Belarus, Ukraine and Russia showed that the maximum injection height was 3–5 km (Evangeliou et al., accepted). In addition, Sofiev et al. (2013) published global maps of emission heights of wildfires that occurred between 2000 and 2012 finding that more than 20% of the smoke was emitted above the boundary layer (~800 m in Chernobyl and Belarus) in Ukrainian and Belarusian forests. However, those fires were of average intensity and started for agricultural purposes. In the present paper, the goal is to study wildfire scenarios. It is well known that crown fires generate sufficient energy to loft smoke plumes above the boundary layer (Lavoue et al., 2000). Case studies have shown that smoke from large fires can be injected to stratospheric altitudes by supercell convection (Fromm and Servranckx, 2003; Fromm et al., 2008). Therefore, in the three scenarios presented here, we account for two different injection patterns: (a) with a maximum injection height at 2.9 km, and (b) at 6.0 km, with 40% of the smoke to be emitted in the free troposphere in both cases. The vertical profile has been adopted from the PRM2 (Plume Rise Model, Paugam et al., 2010) by computing the mean vertical mass profile and applying it to the fire emissions of ^{137}Cs.

The spatial deposition density of ^{137}Cs (Bq m^{-2}) in these forests (known either from measurements or from modeling) is multiplied with the burnt area (m^2) from MODIS and the emission factor (40%), in order to estimate ^{137}Cs emissions after fires. The frequency of the forest fires (timeline) was kept as in the fires of 2010 and the model (LMDZORINCA) was programmed to burn more pixels than the original fires of 2010 representing a surface area of 10, 50 and 100% (2010_scenario_10, 2010_scenario_50, 2010_scenario_100) of the radioactive forests of Ukraine, Belarus and Russia.

2.2. Dosimetric calculation for human and non-human biota

Dosimetric quantities are needed to assess human radiation exposures in a quantitative way. The International Commission on Radiological Protection (ICRP) provides a system of protection against the risks from exposure to ionizing radiation, including recommended dosimetric quantities (Pentreath, 1980). The dosimetric scheme for the calculations of human dose rates was adopted from the WHO (2012) report on Fukushima and includes the most updated approached on dose calculations. External doses from radionuclide deposition represent a significant long-term exposure pathway; hence they were integrated over the first year for Europe. In the present study, the external effective dose from ^{137}Cs deposition on the ground was calculated, together with the external effective dose from the presence of ^{137}Cs in the radioactive cloud (air-submersion) and the internal effective dose from inhalation of ^{137}Cs for the different fire-scenarios studied. In addition, an ingestion contribution of 7% was assumed given the recent experience in Fukushima (Evangeliou et al., 2013b). For the respective doses after the Chernobyl accident only deposition was taken into consideration.

Since the Chernobyl accident, a great challenge in radioecology has been the development of a tool that will be able to record and assess the changes in the population of non-human biota due to effects from ionizing radiation. For this reason, a supporting computer-based software (the ERICA Tool) has been developed (Brown et al., 2003; Larsson, 2004), which guides the user through the assessment process, recording information and decisions and allowing the necessary calculations to estimate risks to selected animals and plants (Larsson, 2008). The results can be put into context using incorporated databases on dose effects, relationships and background dose rates. In the present assessments the Tier 2 scheme was used for dose rate calculations from ^{137}Cs to the terrestrial reference organisms, namely amphibians, birds, bird's eggs, detritivorous invertebrates, flying insects, gastropods, grasses and herbs, lichens and bryophytes, mammals (deer and rat), reptiles, shrub, soil invertebrates (worms) and trees.

2.3. Lethal and incidence risk calculation to humans from radiation cancer

The LNT-model of human exposure was used to calculate radiological health effects, similar to the Chernobyl accident (EPA, 1999; ICRP, 2005). The model assumes that each radionuclide's disintegration has the same probability of causing cell transformation, and that each transformed cell has the same probability of developing a tumor. Although the LNT-model has been employed extensively in radiation safety (NRC, 2006; UNSCEAR, 2010), several arguments about its validity and response at low doses still remain unresolved. Most of them provide evidence that the risk might not be linear, showing a decreasing or increasing trend, or being even hormetic (beneficial at low doses) (e.g. Cuttler, 2010; Tubiana et al., 2009). This is mainly because epidemiological studies have only considered doses above 100 mSv showing a statistically significant increase in stochastic cancer risk, although at doses below 100 mSv significance or lack thereof has not been observed. On the other hand, supporters of the LNT-model claim that the difficulty in attributing a small number of cancers to low doses does not necessarily indicate an absence of risk (Hoffman et al., 2012).

A radiogenic cancer risk model defines the relationship between radiation dose and the subsequent force of death (or incident) attributable to that dose. Death risk is defined as an estimate of the risk to an average member of the population of dying from cancer over its lifetime. Incident risk is the risk of experiencing radiogenic cancer during a person's lifetime, whether this cancer is fatal or not. Inhalation, ground deposition and air-submersion exposure pathways were considered for ^{137}Cs and its decay product ^{137m}Ba, respectively (ICRP, 1995). The excess lifetime cancer death and incident risk from each exposure pathway (below for inhalation) were calculated by the following equation (Ten Hoeve and Jacobson, 2012):

$$R_s = \sum_i \sum_j \left\{ P_{ij} \left[1 - \exp\left[- r_s \sum_t \left(I_R \left(A_{i,j,t,s} - A_{t,d}, 0 \right) \right) \right] \right] \right\} \quad \text{Eq. (1)}$$

where

R_s is the total number of lifetime cancer deaths or incidents due to species s over all times t (life expectancy of the European population is 75.1 years, UNPD, 2014) and grid cells i, j,

P_{ij} is the 2010 population in each grid cell i, j (NASA, 2013),
r_s is the relative cancer death or incident risk coefficient for species s expressed in units of Bq^{-1} (or m^2 Bq^{-1} and m^3 Bq^{-1} for ground-level and external atmospheric exposure) from EPA (1994),
I_R is the inhalation rate (17.8 m^3 day^{-1}, EPA, 1999),
$A_{i,j,t,s}$ is the species' concentrations in each grid cell i, j at time t, and
$A_{t,d}$ is the threshold concentration below which no visible effect occurs (for the LNT-model is zero by default).

External ground deposition and external atmospheric exposure were calculated using the same equation without the respective internal rates (I_R). The shielding effect inside structures was also taken into account by assuming a 30% reduction in exposure from particulate ^{137}Cs and its decay product for 12 h each day when people are assumed to be indoors (Price and Jayaraman, 2006). It has been found that ^{137}Cs resided in the atmosphere for 2–3 months after large releases (e.g. Fukushima, Masson et al., 2011; McMullin et al., 2012; Paatero et al., 2012). Therefore, external atmospheric and internal inhalation exposures were negligible 3 months after and only ground deposition exposure was significant the following years.

Many researchers do not accept the LNT-hypothesis for risk assessments, due to the lack of a threshold value, below which no visible effects would be observed. For this reason, in the present risk assessment we apply a DDREF (Dose and Dose Rate Effectiveness Factor) of 2 (EPA, 1999; UNSCEAR, 1993). In general, epidemiological estimates of radiation-related overall and site-specific cancer risks (except for leukemia) are statistically consistent with a linear dose–response relationship (ICRP, 2005). For the same reasons that data restricted to low doses tend to be uninformative about radiation-related excess risk, this apparent linearity does not rule out, on statistical grounds, the possibility of increased, decreased, or even no excess risk per unit dose at very low doses. Therefore, the linear-estimated excess lifetime risks are often divided by a DDREF at low doses and low dose rates as a method to substitute the uncertain threshold.

3. Results

3.1. Transport and deposition of the radioactive fallout

The prevailing atmospheric concentrations of ^{137}Cs during its transport in the three wildfire scenarios (2010_scenario_10, 2010_scenario_50, 2010_scenario_100) can be seen in Fig. 1 for 8 August, where the maximum release in the middle of summer took place. This was a result from several fires that occurred for two almost consecutive months (8 July–17 August) inside contaminated regions, due to an intense heat wave caused by atmospheric blocking (Matsueda, 2011), which began in mid-June, intensified around 18 July and ended with a cold front passage in 18 August. Two maps for each scenario are presented, due to the aforementioned different maximum injection altitudes at 2.9 and 6.0 km used in the model (Fig. 1). The range of ^{137}Cs activity concentrations in the atmospheric aerosol in the first scenario (2010_scenario_10) is only significant mostly for the local areas around the contaminated forests, when concentrations are in the range of few tens of mBq per m^3. This is not the case in the most intense scenarios, where the plumes reach North Europe and Central Russia with maximum concentrations up to three orders of magnitude higher.

During the 11–21 July period, prior to the fire peak, air parcels reaching Central Russia were generally from the north to west and MODIS showed no significant fires in the vicinity of this transport pathway. During 22–29 July winds reaching Moscow shifted southeasterly flowing over regions of significant fire activity. Then an increased number of fires with greater intensity occurred in the three radioactively contaminated forests and an anticyclonic pattern began to form, which persisted at all pressure levels. Fires continued to be numerous and intense. Air was circulated and re-circulated bringing ^{137}Cs and by-products from the wildfires. During 1–10 August, air generally entered Moscow from the south going to the north and increasing activity concentrations over Sweden and Finland. On the other hand, ^{137}Cs injected at a higher pressure level was dispersed faster moving to the south-east (across the Caspian Sea) (see Fig. 1). The beginning of the post-fire period in 19 August coincided with the end of the heat wave. Numerous fires in Eastern Europe were still detected by MODIS, but the fires over contaminated forests had diminished except for two incidents at the beginning of September and the end of October (Fig. 2).

Fig. 2 depicts the atmospheric burden of ^{137}Cs in our simulations (for the year 2010) and it is compared with Chernobyl and Fukushima accidents as seen by the same model. At a first glance, the differences in ^{137}Cs transport, due to the two vertical schemes, seem to be insignificant. Aside from the patterns of transport, found to be similar, the longer residence of ^{137}Cs in the atmospheric aerosol (as a result of a release at a higher vertical level) causes an expected high dilution due to the larger dispersion at longer distances. This is apparent in the prevailing activity concentrations in Sweden and Finland that are one order of magnitude higher when ^{137}Cs is released at a lower altitude. Fig. S1 (Supporting information — SI) depicts an example of the prevailing activity concentrations of ^{137}Cs on 30 April 1986 (Chernobyl), in comparison with those resulting from the three scenarios (emitted at maximum height of 6.0 km). Undoubtedly, in the first case, ^{137}Cs dominated atmospheric fallout with concentrations up to 6 orders of magnitude higher than those presented in the fire scenarios. Nevertheless, if half or all of the contaminated forests burned, concentrations in the range of Bq per m^3 could reach large populated centers, such as Moscow, or cover all of Belarus. Fig. S2 (SI) shows how far from the source the plume would reach for the different scenarios and injection heights. Hence, North America would receive a bulk of ^{137}Cs ranging between 0.1 and 1 mBq m^{-3}, whereas North Africa would experience a maximum of 5 mBq m^{-3} and Central Asia one of up to 50 mBq m^{-3} (decreasing to the east). Just after Chernobyl, the activity concentrations of ^{137}Cs in New York were around 9.5 mBq m^{-3} (Feely et al., 1988) and 10 times higher in Canada (Joshi, 1987), whereas traces had been found in Japan (Aoyama et al., 1986). In addition, from the recent accident in Japan, the CTBTO (Comprehensive Nuclear Test Ban Treaty Organization) reported ^{137}Cs concentrations to be around 1 mBq m^{-3} in North America, 3 orders of magnitude less in Africa and between 0.1 and 1 mBq m^{-3} in Central Asia (Christoudias and Lelieveld, 2013).

The cumulative deposition of ^{137}Cs for the year of the simulations (2010) and for the three fire scenarios with the emissions taking place at 6.0 km can be seen in Fig. 3, whereas the extend of deposition can be seen in Fig. S3 (SI). In Fig. 3 the cumulative deposition of ^{137}Cs after the Chernobyl accident can also be seen simulated by the same model for 1986 adopted from Evangeliou et al. (2013a). Bergan (2000) in the first complete study about ecological loss of ^{137}Cs reported that "the calculated effective half-lives of radiocesium in the surface soil layer vary across the sites from 10 to 30 years which is equal to the physical half-life of ^{137}Cs". Effective half-life of ^{137}Cs combines its physical decay and also its ecological half-life (which includes all environmental removing processes, such as vertical migration, runoff to large reservoirs, soil erosion etc.). Therefore, the data in Fig. 3 have been corrected for 2010 using an effective half-live of ^{137}Cs of 10 years (Bergan, 2000). The map is used here to compare what is still deposited in Europe from a massive deposition (Chernobyl), with the redistribution and deposition of ^{137}Cs after wildfires. Although smaller fires (such as those of 10% of the contaminated area) might be extinguished by firemen, intermediate or large fires would definitely be hard to fight in the abandoned contaminated forests of Chernobyl, Belarus and Russia, where little forest management occurs (Zibtsev et al., 2011). Our estimates show that 1 to 90 kBq m^{-2} can be re-deposited over Europe in one fire year affecting an area of several million inhabitants. The highest deposition would be observed in the pixels of the forests, where deposition is expected to

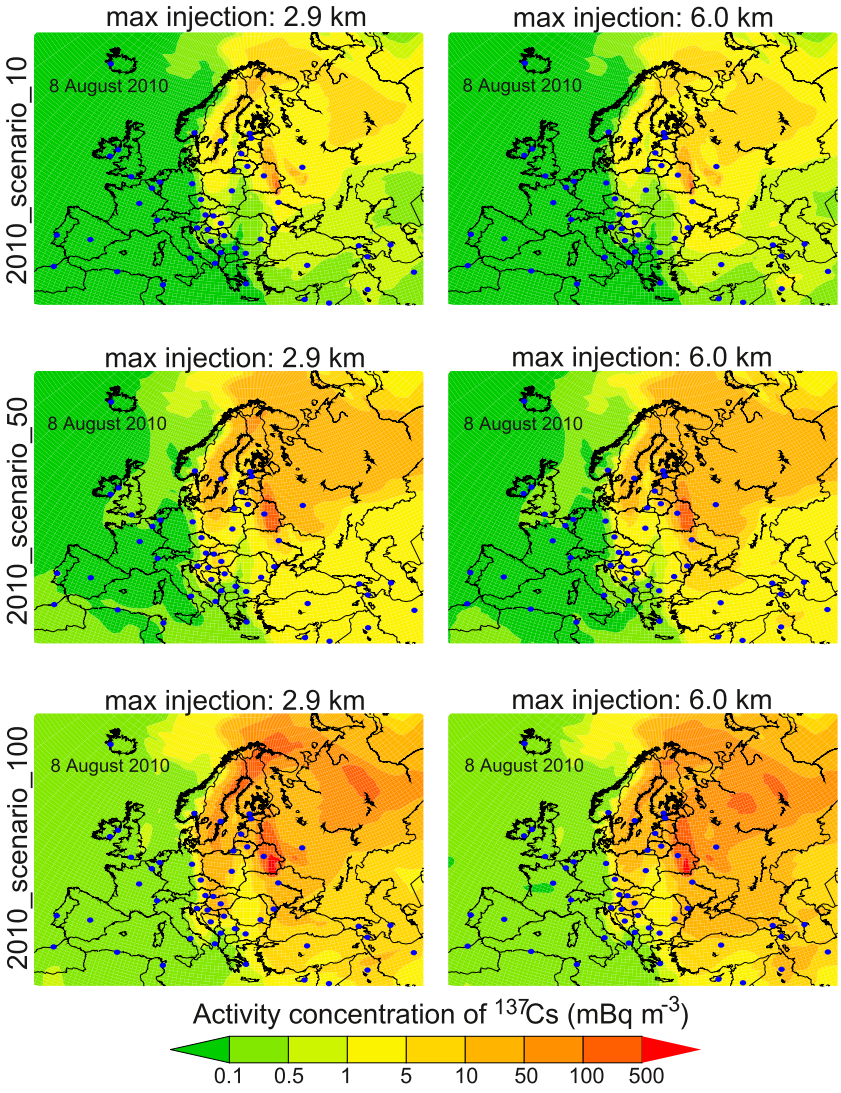

Fig. 1. Example of aerosol activity concentrations of ^{137}Cs in ground-level air (mBq m^{-3}) in Europe during the largest release (emissions for 10 consecutive days) on 8 August 2010 for the three different fire scenarios (2010_scenario_10, 2010_scenario_50, 2010_scenario_100). Two different figures are presented for maximum injection at 2.9 and 6.0 km, respectively. The blue dots represent the location of the metropolitan areas. (For interpretation of the references to colour in this figure legend, the reader is referred to the web version of this article.)

exceed 5 kBq m^{-2}. These amounts are somehow significant if one takes into consideration that more than 3000 kBq m^{-2} (maximum values) still exist around Chernobyl.

3.2. Dosimetric calculations and lifetime risks for the population

Another significant question that needs to be addressed is what the increase of the dose-rate would be following the studied scenarios. We provide effective dose estimations of the public resulting from exposure in 2010 for the different fire scenarios (Fig. 4). The methodology used to calculate the doses relies on the most recent dosimetric and biokinetic models for adults (although estimates on different population subgroups are possible). The dosimetric scheme considers all major routes of exposure: (i) air-submersion, (ii) deposition and (iii) inhalation of ^{137}Cs, plus a 7% contribution from the resulting presence of ^{137}Cs into different foodstuffs (ingestion). The assessment contains a number of assumptions (e.g., fallout composition and dispersion, time spent indoors/outdoors, and consumption levels). The cumulative effective dose from exposure to ^{137}Cs (for the first year) would be 0.0001 to 0.01 mSv in the first scenario, where 10% of the area burns mostly affecting the adjoined areas, up to 0.05 mSv, if half of the contaminated forests were burned and up to 0.1 mSv if the whole area was burned. These values are below what happened after Chernobyl in Europe or what has been remained from Chernobyl in 2010 (applying an effective half-life of 10 years, Fig. 4). Moreover, only the extreme scenario affects all Europe, whereas when 10 or 50% of the area burns, low contribution to the western European countries can be seen.

The experience of Chernobyl and Fukushima accidents has shown that the effective doses will decrease within the first year after a big release mainly due to radioactive decay of short-lived radionuclides, as well as due to the exponential decrease of the atmospheric burden of volatile compounds (such as ^{137}Cs), which in turn, will result in a rapid decrease of the corresponding effective dose (inhalation and air-submersion doses can be neglected the following years). In addition, the dose from exposure to ground-deposited ^{137}Cs is expected to decrease during the following decade due to vertical migration into the soil (Bunzl et al., 1992). The shielding effect of soil is an important factor that will further reduce obtained doses the following years. For example, about 30% of the effective dose has been estimated to decrease during the first year, while about 70% during the first 15 years (Golikov et al., 2002).

Chronic radiation exposures (occupational) are generally associated with lower cancer risks than acute ones (accidents) for the same total dose (Little et al., 2009). Good evidence for an increase in cancer risk

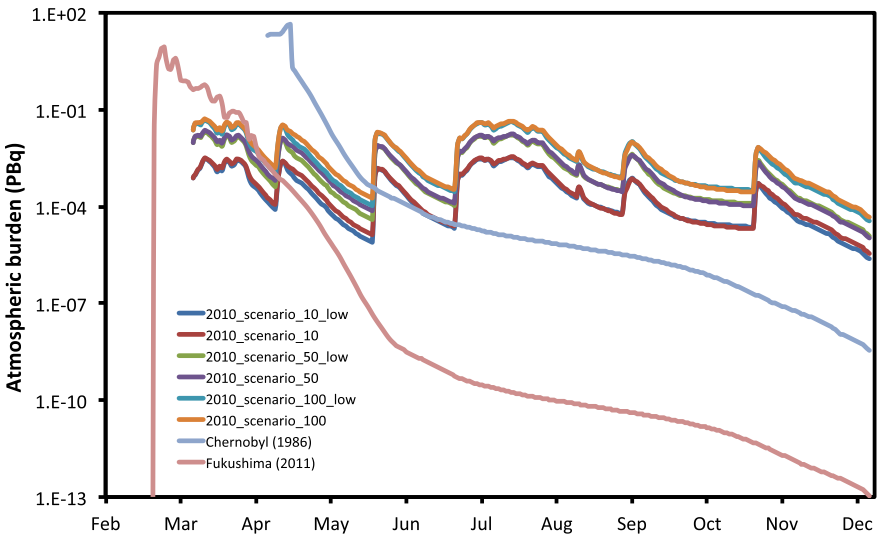

Fig. 2. Atmospheric burden of ^{137}Cs (PBq) throughout the simulated year for the three scenarios (2010_scenario_10, 2010_scenario_50, 2010_scenario_100) and the two vertical parameterizations, with "low" denoting the lower level injection (2.9 km), and the rest was the highest one (6.0 km). For comparison, the same burden for the Chernobyl (1986) and Fukushima (2011) accidents (adopted from Evangeliou et al., 2013a; 2014b) are also shown simulated by the same model, in order to highlight the magnitude of the emissions during the studied scenarios.

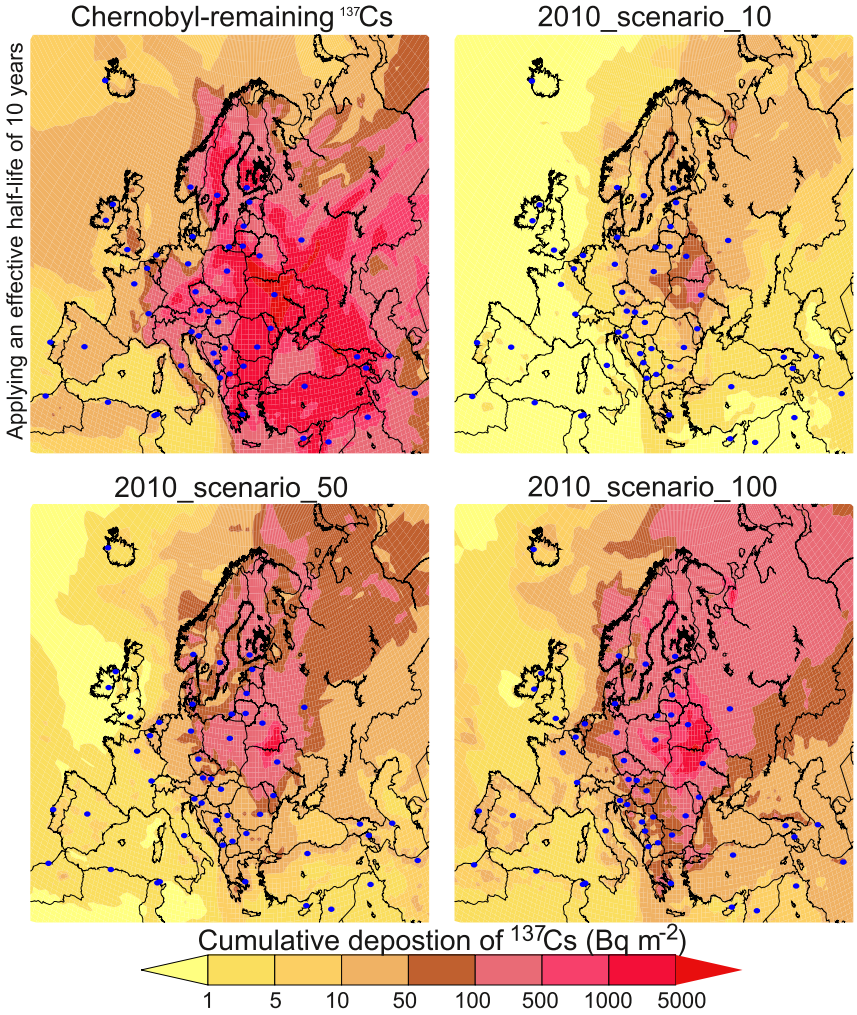

Fig. 3. Deposition density of ^{137}Cs (Bq m^{-2}) integrated for the year 2010 following the three fire scenarios (2010_scenario_10, 2010_scenario_50, 2010_scenario_100) for a maximum injection height of 6.0 km. For comparison, the remaining ^{137}Cs deposition in 2010 is provided simulated by the same model (adopted from Evangeliou et al., 2013a) applying an effective half-life of 10 years(Bergan, 2000).

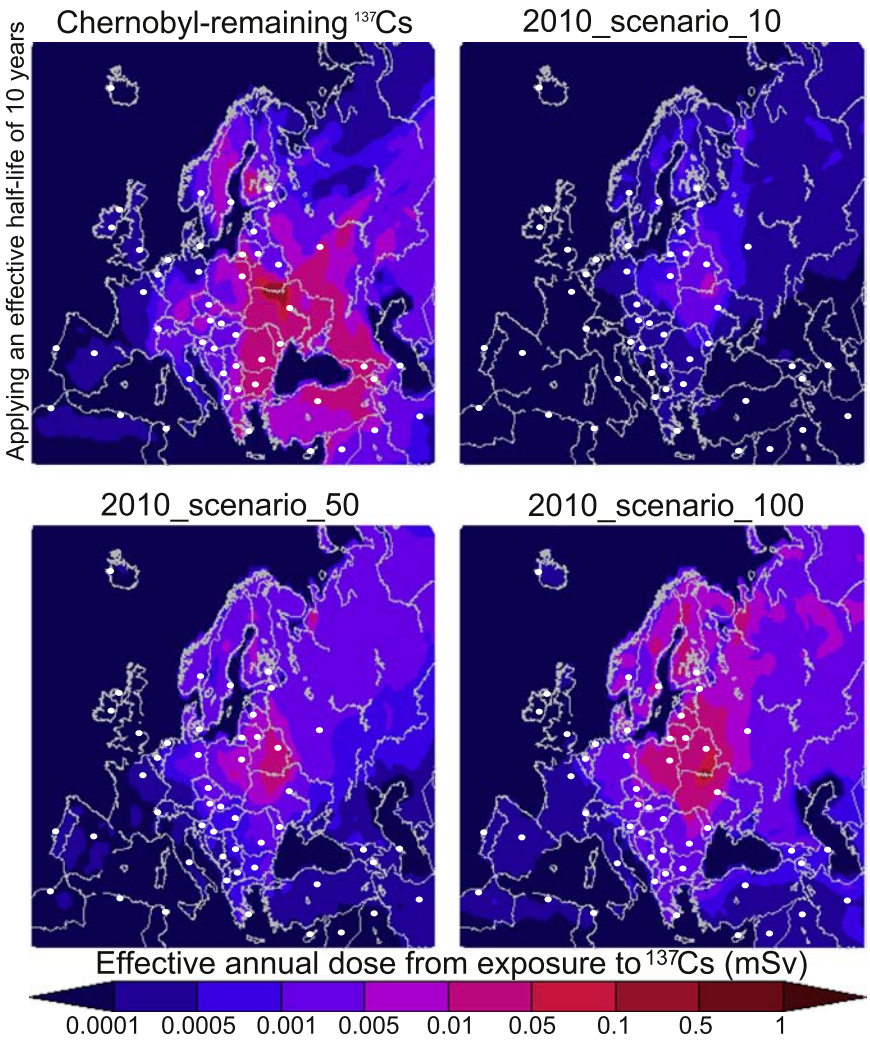

Fig. 4. Cumulative effective dose from ^{137}Cs exposure in Europe for the first year following the fire scenarios. The effective dose from deposition exposure to the Chernobyl-remaining ^{137}Cs is also given (adopted from Evangeliou et al., 2013a). The white dots denote the location of the metropolitan areas.

is shown for acute doses greater than 100 mSv, whereas chronic exposures of this dose level present a much higher risk (Boice, 2012). The linear dose–response relationship used here is a possible descriptor of low-dose radiation oncogenesis, although different shapes may well explain dose–response relations. About one fifth of people worldwide and one third of people in heavy-industrialized regions are diagnosed with cancer during their lifetime (IARC, 2008). Radiation can induce cancers that are indistinguishable from cancers resulting from other causes. Most population-based cancer risk estimates come from the Japanese atomic bomb survivors, as well as from other sources of radiation exposure, where useful epidemiological data are available (e.g. past accidents, medical and environmental exposures). Nevertheless, although a large number of solid cancers have been observed after such exposures, the most frequent radiation-related cancer is leukemia (Tsushima et al., 2012).

The excess lifetime cancer mortalities from ^{137}Cs exposure after the three scenarios (applying a DDREF of 2 in Eq. (1)) are depicted in Fig. 5 for the gridded population of 2010, together with the respective ones just after the Chernobyl accident in 1986. The average life expectancy in Europe is 75 years (OECD, 2012), and this value was used here. Moreover, we compare cancer risks from fires with the respective ones from the remained deposited ^{137}Cs assuming an effective half-life of 10 years (Bergan, 2000). The pathways of deposition, air-submersion and inhalation were taken into consideration, whereas food ingestion was assumed to contribute around 7% (such as in the dose calculations) to the total risk. For the risk calculations of the Chernobyl-remaining ^{137}Cs over Europe, deposition exposure was only taken onto account. It is evident that when 10 and 50% of the contaminated forests were burned, very few deaths can be predicted (Fig. 5). More specifically, 1–4 deaths per pixel can be seen (0.45° × 0.51°) mostly around the contaminated forests of Ukraine and Belarus, when 10% of the area burns affecting Ukraine and Belarus, as well as Poland. On the other hand, when 50% of the forests were burned, several central European metropolises are affected including Kiev, Minsk, Warsaw and Berlin (1–4 deaths per pixel). Finally, in an extreme fire-scenario the highest risks for the capitals of Ukraine, Belarus and Poland are calculated, while effects on the population of western European capitals may be observed (Fig. 5).

3.3. Doses and observations on animal populations

The ERICA Tool was applied to the selected reference organisms of the terrestrial ecosystem (amphibians, birds, bird's eggs, detritivorous invertebrates, flying insects, gastropods, grasses and herbs, lichens and bryophytes, mammals (deer and rat), reptiles, shrub, soil invertebrates (worms) and trees). Fig. 6 (upper panel) depicts soil and air activity concentrations of ^{137}Cs at the surface of the contaminated forests averaged every 5 days for the three fire scenarios, as well as for Chernobyl and Fukushima. The horizontal black line denotes the background soil concentration averaged for the contaminated forests of Chernobyl,

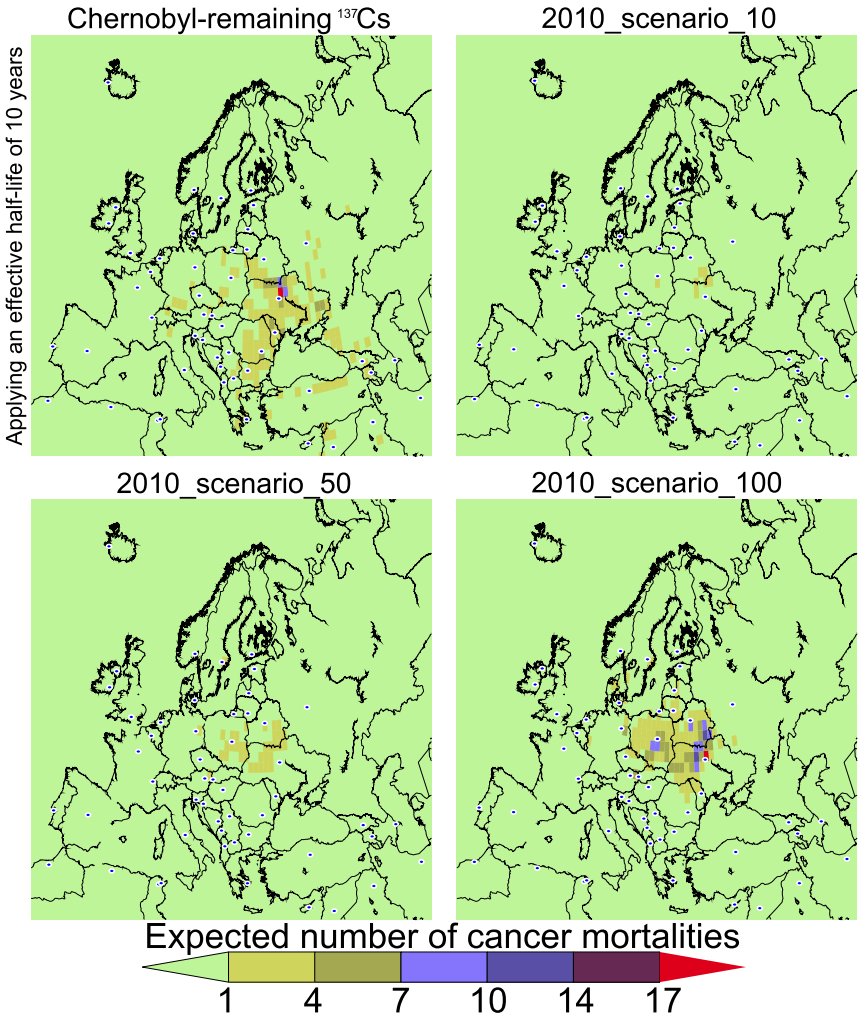

Fig. 5. Excess lifetime cancer mortality from all exposure pathways to ^{137}Cs (air-submersion, deposition, inhalation and 7% contribution from ingestion). The same mortality rate is also given for the Chernobyl-remaining ^{137}Cs from deposition exposure only (correcting with an effective half-life of 10 years, Bergan, 2000) (adopted from Evangeliou et al., 2013a). All rates have been applied to the European population of 2010 to obtain a number of individuals that are expected to die from cancer. The white dots represent the location of the metropolitan areas.

Belarus and Russia. Soil concentrations were calculated from deposition densities provided by our model (Bq m^{-2}) applying a conversion factor of 228 kg m^{-2} based on 542 measurements of soil concentration and deposition density in the CEZ and Belarus (Kashparov et al., 2003). Soil concentrations calculated for the three fire scenarios were added to the background soil average soil concentration estimated by the same database (Kashparov et al., 2003) (Fig. S4). Hence, 5-day average dose rates (μGy h^{-1}) were calculated for the reference organisms exposed to this environment. For comparison, the doses from the Chernobyl and Fukushima accidents were also calculated (Fig. 6) for the same organisms that are assumed to live in the contaminated forests, as well as in the FEZ (Fukushima Exclusion Zone). The horizontal line denotes the screening dose-rate limit of 10 μGy h^{-1}.

Internal exposure had higher contribution to total doses in birds, lichens and bryophytes, mammals (deer and rat), reptiles and shrubs, while the opposite was found for the rest. Total dose-rates for the selected reference organisms ranged from 0.5 to 5.3 μGy h^{-1}, which are below the screening dose of 10 μGy h^{-1} that could harm the abundance of a population. These values are far below the doses that the selected organisms would have selected during the accident of Chernobyl in 1986 (2.7–24.5 μGy h^{-1}) or the recent accident in Japan (1.0–9.4 μGy h^{-1}). It is noteworthy that even after Chernobyl, where concentrations were orders of magnitude higher than those observed during the three scenarios, absorbed doses exceeded screening value only for lichens and bryophytes, mammals (deer and rat), reptiles and shrubs, whereas invertebrates were slightly below the screening level. In contrast, just after Fukushima only mammals and reptiles could face significant danger.

4. Discussion

4.1. Are major fires in radioactively contaminated areas identical to accidents?

The major question of this study is if an uncontrolled fire inside the Chernobyl-contaminated forests of Ukraine, Belarus and Russia would be likely to cause such a release that would be identical to a major nuclear accident. According to Fig. 2, the releases of ^{137}Cs, if 10% of the area burned, would be 0.29 PBq ($\times 10^{15}$ Bq), whereas if fires affected half of the contaminated regions, it would be 1.6 PBq. Finally, for the extreme wildfire scenario of the whole area burned, the overall amount of ^{137}Cs emitted in the atmosphere would be 4.2 PBq. These releases are lower than those after accidents rated as 7 in INES (International Nuclear and Radiological Event Scale, IAEA, 2013), such as Chernobyl (85 PBq, De Cort et al., 1998), or the recent accident in Fukushima (37 PBq, Stohl et al., 2012). However, they are at the same level or higher than accidents rated as 6, such as the Kyshtym disaster, which

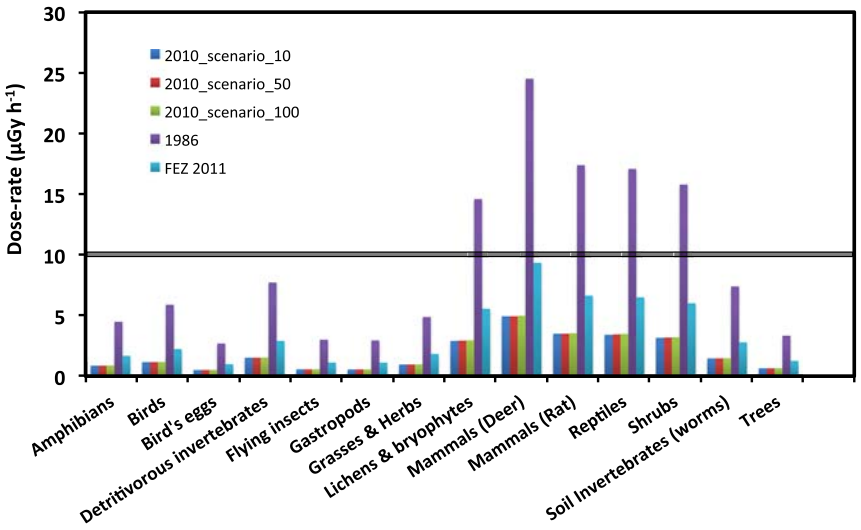

Fig. 6. Dose-rates received by selected reference organisms (5-day averages) that live and reproduce in the contaminated forests of Chernobyl, Belarus and Russia. The horizontal black lines denote the screening dose-rate (below which no visible effects of radiation to reference organisms can be observed).

resulted in the release of 13 TBq of ^{137}Cs ($\times 10^{12}$ Bq, Jones, 2007) or 5, such as Windscale, which released 22 TBq of ^{137}Cs (Cooper et al., 2003).

Of course, the significance of a radioactive release is not only based on the release of one radioisotope, but also based on the total amount, and how dangerous they are (e.g. type of emission during decay, half-life). According to De Cort et al. (1998) 10.9 EBq ($\times 10^{18}$ Bq) of fission products were released after Chernobyl, of which 80% were deposited in Europe. Thirteen out of nineteen radionuclides, which were released in the range of PBq, presented half-lives from days to 2 years meaning that they have been lost due to decay nowadays. From the remaining, four out of six are refractory elements ($^{238–240}$Pu and traces of ^{241}Am) that have been "trapped" in the CEZ. The last two are ^{137}Cs (volatile element) and ^{90}Sr, an element with intermediate volatility, that present half-lives of around 30 years. According to measurements (NRU, 2011) and our simulations, around 10 PBq of ^{137}Cs and 5 PBq of ^{90}Sr remain in contaminated areas. Taking into account that most refractory elements constitute the local fallout and therefore cannot go far, the most dangerous radionuclides are ^{137}Cs and ^{90}Sr. This means that the aforementioned releases after a major fire event in the contaminated forests of Chernobyl, Belarus and Russia could reach an INES level of maximum 6, which can be considered a serious accident (the INES scale intends to be logarithmic and each level represents an accident approximately ten times more severe than the previous level).

4.2. Is there a realistic risk for the European population?

In order to assess the importance and impact of the estimated doses to humans, they are compared with exposures arising from other sources. The United Nations Scientific Committee on the Effects of Atomic Radiation (UNSCEAR) estimated the global average effective dose per person from all natural and artificial sources of radiation in the environment to be approximately 3.0 mSv per year (UNSCEAR, 2008a). About 80% of the annual radiation dose that a person receives is due to natural radiation from cosmic rays, the earth, and naturally occurring radionuclides in food and drink (2.4 mSv per year). Due to geological differences, people may receive annual effective doses significantly higher than the global average. The most significant artificial sources of human exposure are radiological medical investigations and treatment (UNSCEAR, 2008b).

According to the dose calculation for the first year (2010), the obtained doses from the contaminated forests fires in Chernobyl, Belarus and Russia are higher that those obtained from a simple medical exposure (e.g., dental X-ray 0.005 mSv or chest X-ray 0.02 mSv) and can be compared with those of cosmic rays after transoceanic flight. However, the dose estimates might not reflect the overall situation especially near the contaminated forests. This is because we do not account for the long-lived radionuclides deposited there since Chernobyl. As mentioned previously, after the accident, the heavy debris (consisting of transuranium elements) dominated the local fallout and was deposited in the CEZ, as well as in parts of the Belarusian forests (some kilometers north of the NPP), as a result of the heaviness of elements such as $^{238–240}$Pu and ^{241}Am. We expect that there must be some contribution to the total dose from these elements, although they cannot reach far. In addition, those doses reported here have been calculated for the first year of the fire events (2010). This means that the most severe exposure pathway (inhalation) will be negligible in the following years (if no new fire events occurred). Nevertheless, MODIS satellite has recorded an increasing trend of forest fires in Chernobyl's forests showing that the redistribution of ^{137}Cs will not occur in only one year per lifetime of the population.

The question that now arises is how plausible it is for fire events to occur inside contaminated forests. Evangeliou et al. (accepted) reported the risk of wild fires in these forests. They found that vegetation type distribution, interannual variation of different fuel amount and fuel moisture content affect fuel continuity and the ability of a fire to spread during a large event. The relationship between extreme fire years with an increasing summer drought may potentially result in more extended burned areas. Grassland fields appear to be the most fire prone areas in Eastern Europe, and forest patches large enough to carry out extreme fire events. They showed significant forest extensions inside the restricted regions since 1986, suggesting an increasing continuity in forest patches and in turn large fire risk. Litter accumulation in the contaminated forests has increased since 1986 as a result of radiation levels that decrease plant decomposition rates (Mousseau et al., 2014). Finally, some future projections of burned area and litter accumulation presented in the same work suggest that intense fire years in these forests are frequently expected (e.g. 2015–2025, 2037–2041, 2067–2100).

In certain cases, cancer mortalities from fires seem to be in the same range as from the Chernobyl-remaining ^{137}Cs. However, it should be noted that for the calculation of the risk from Chernobyl the pathway of ground-deposition has only been taken into account. This is because air-submersion and inhalation exposures are negligible (even one year after) and food-ingestion is well-controlled in Europe nowadays (with the possible exception of some fruits). Internal

pathways (inhalation and ingestion) are the most dangerous exposures, although deposition may play an important role as a chronic parameter. The number of projected deaths (and cancer incidents, Fig. S5 — SI), however, is still considerably smaller than the estimated ones for the Chernobyl-remaining ^{137}Cs (Fig. 5).

The total lifetime cancer incidents during the three studied fire scenarios range between 23 and 238, of which 15–169 are expected to be fatal. The same incidents and mortalities after Chernobyl are estimated to be between 5800 and 7300, whereas from the Chernobyl-remaining ^{137}Cs 348 and 285 (adopted from Evangeliou et al., 2013a) accounting deposition exposure only. In addition, 290–810 incidents and 200–500 mortalities have been estimated from exposure to ^{137}Cs after the Fukushima accident (adopted from Evangeliou et al., 2014b). According to OECD (2012), in 2010 there were 150–200 deaths from all cancers per 100,000 individuals in Europe. This gives a total number of fatalities between 1.1 and 1.5 million of fatalities. From a first look, the values that resulted from the fire scenarios are somehow comparable to those observed after Fukushima, although emissions from Fukushima were 1–3 orders of magnitude higher (Fig. 2). The main explanation is that 80% of the fallout after Fukushima was deposited in the oceans, with the rest in continental areas. On the other hand, we estimate that more than 90% of the fallout of ^{137}Cs emitted after the three scenarios will finally be deposited in Eurasia (Fig. S2 — SI). Finally, the exposure pathway of inhalation, which contributes the most to the final risk, remains enhanced during the whole year 2010, as a result of the multiple fire events, which keep airborne ^{137}Cs activity concentrations high over Europe.

4.3. Validation and uncertainties

In order to evaluate the response of our model to such kind of hypothetical emissions, we studied the fires of 2010 in all forests of Ukraine, Belarus and Russia as they actually happened and recorded by NASA's satellites. For this reason the area burnt was obtained from MODIS, the deposition density of ^{137}Cs was calculated from Evangeliou et al. (2013a) correcting for an effective half-life of ^{137}Cs of 10 years (Bergan, 2000), whereas an emission factor of 40% was accounted for, as in the fire scenarios. The results were compared with observations from the CTBTO network (Dubna, Russian Federation and Yellowknife, Canada) and modeling results reported by Strode et al. (2012). The spaghetti plots of the comparison of the surface concentration of ^{137}Cs can be seen in Fig. 7. The normalized mean bias (NMB) of our model (LMDZORINCA) was estimated to be 65%, in contrast to 42% estimated for Strode et al. (2012). However, the percentage of sites with deviations of the modeled concentrations from the observations less than a factor of 2 was 56% using our model, whereas the same parameter was 50% as reported in Strode et al. (2012) and the correlation coefficient of a linear fitting was slightly improved (0.45). A Student's T-Test was also performed to compare our results with those of Strode et al. (2012) achieving a high probability ($P \approx 1$), which shows that the two datasets cannot be distinguished. Small differences can be attributed to the different methodology used to estimate surface activity concentrations of ^{137}Cs. Strode et al. (2012) simulated concentrations of ^{137}Cs by multiplying the modeled POM tracers by the ratio of ^{137}Cs emission to

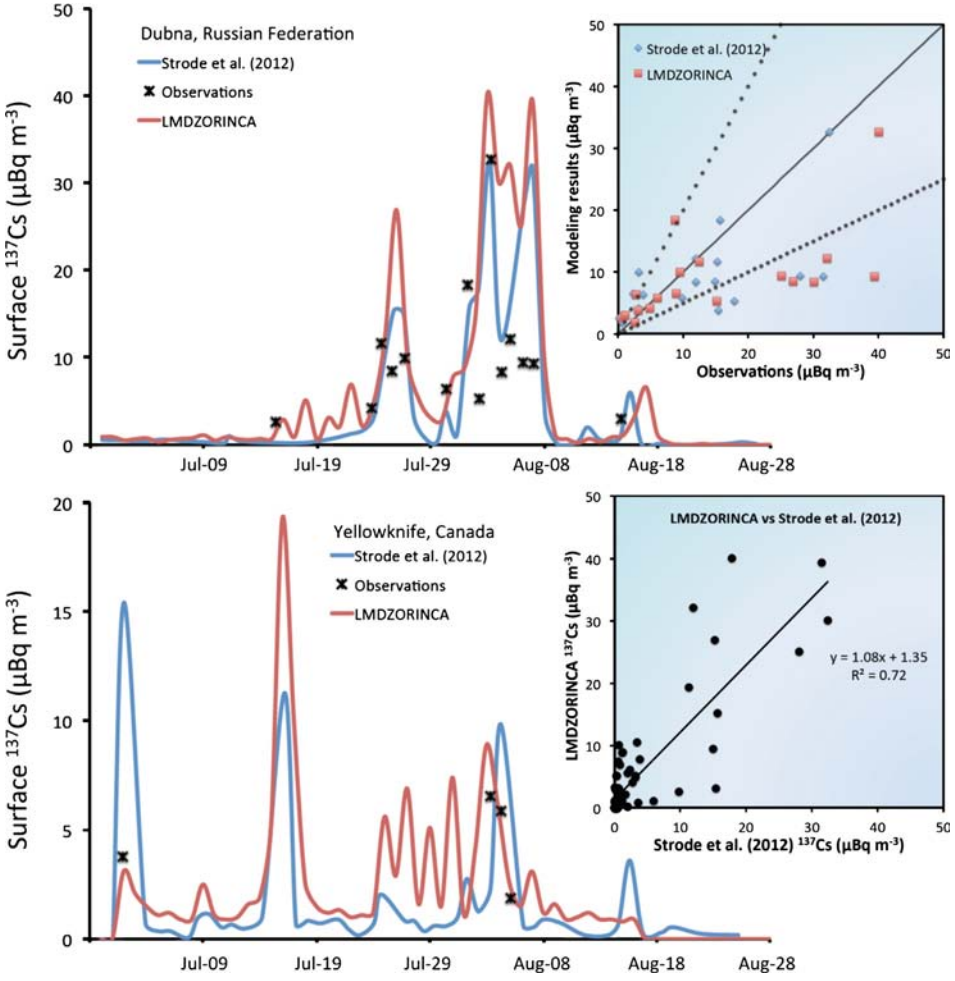

Fig. 7. Comparison of the LMDZORINCA model was used to simulate fire scenarios with the calculations of Strode et al. (2012) and CTBTO observations for the original forest fires of 2010. Our model computed surface concentrations of ^{137}Cs very efficient recording the arrival times of the plume to each station and the main peaks as well, while high consistency was achieved with observations and with the modeling results reported by Strode et al. (2012).

POM emission from biomass burning ($=0.23$ kBq kg^{-1}) assuming that particles containing ^{137}Cs undergo the same transport and neglecting radioactive decay. On the contrary, we used MODIS area burnt, modeled deposition densities of ^{137}Cs in the area and an experimental emission factor of ^{137}Cs. Nevertheless, LMDZORINCA models reproduced well the arrival times of the plume, the levels of surface ^{137}Cs concentrations and the major peaks. It is noteworthy that although fires of such large extent as in the present scenarios have not been happened yet in Chernobyl-contaminated forests, 2010 fires burnt 9% of the forest area according to MODIS. Therefore, a study of these scenarios does not necessarily constitute exaggeration, as it seems there is a certain possibility for large fires to occur in the area.

The uncertainties of our estimations strongly depend on the methodology used. Regarding MODIS area burnt, Urbanski et al. (2009) reported that the uncertainty could rise up to 40% depending on the pixel and time resolution, the fire size etc. In addition, although the deposition density provided by the simulation of the Chernobyl accident (Evangeliou et al., 2013a) has been validated using the REM database (De Cort et al., 1998), there is no unique study on effective half-life variations in Europe that could certify that the value used here (10 years) was realistic and represents all Europe. Moreover, the emission factor of ^{137}Cs is strongly dependent on the type of the fuel and the prevailing temperature of the flame during a fire. Assuming that the whole pixel is covered by biomass, the emission factor may range from 20 to 100%. Hence, uncertainties can increase by up to more than 50% in our estimations, which are propagated to the health assessment of animal and human populations.

4.4. Environmental consequences

The environmental consequences of forest fires and the resulting redistribution of radionuclides may also have implications for organisms other than humans. Although the predictions based on the ERICA Tool revealed elevated, but still relatively weak effects even under worst-case scenarios, these effects may not be the whole story. Species with high metabolic rates such as small mammals like rodents and shrews and many birds may ingest disproportionately large amounts of radionuclides (Møller and Mousseau, 2006). Organisms placed high in the food chain accumulate large amounts of radionuclides with effects that go beyond the direct effects of radiation (Møller and Mousseau, 2008, 2009). A particularly dramatic example of indirect effects of redistribution of radionuclides is the ability of many fungi to concentrate radionuclides by several orders of magnitude (Møller and Mousseau, 2006, 2011). Species that consume such fungi not only insects, slugs and snails, but also larger species like roe deer and wild boar have been found to have high dose levels even in areas far away from Chernobyl such as in areas of Finland, Sweden and Norway and, also, in Austria and Italy (Møller and Mousseau, 2013). Interestingly, humans in contaminated areas around Chernobyl and elsewhere in the region acquire a large fraction of their total exposure to radionuclides from consumption of fungi (Shuton et al., 1996). Thus, the effects of bioaccumulation in humans may resemble the patterns observed in roe deer and wild boar. Redistribution of radionuclides across Eastern Europe and Russia might have their major effect not through exposure to radiation from redistributed radionuclides, but through consumption of fungi that constitute a major stable of the human diet in these parts of the world.

5. Conclusions

Forest natural succession in Chernobyl has been increased since 1986, as a result of the intense radioactive contamination and the subsequent evacuation of large areas mainly in Chernobyl (Ukraine) and Belarus. Trees nowadays cover more than 70% of these areas, and taking into consideration the predicted trends of climate change, increased risk of wildfires can be concluded in these forests. In the present paper we study the implications of such forest fires by examining three scenarios in the Chernobyl-contaminated forests of Ukraine, Belarus and Russia: (a) 10%, (b) 50% and (c) the whole forest-area being affected by intense fire events for the meteorological conditions and the temporal distribution of fires of the year 2010 (as recorded from MODIS). Fires of small extent have already happened in the area (e.g. 2002 fires burnt almost 9% of these forests). With the projected climate change evolving in the area and given the social and politico-economical situation in Ukraine nowadays, extended forest fires pose as a realistic scenario.

According to our estimates, significant amounts of ^{137}Cs can be transferred to largely populated centers, especially in Central and East Europe. It is noteworthy that 0.3 to 4.5 PBq (available at the forests of Ukraine, Belarus and Russia) is expected to migrate over Europe after only one massive year! Large fire events in contaminated forests may not imply a “major nuclear event”, such as those of Chernobyl and Fukushima, but they can be classified as “accident with local or wider consequences”, or even as a “serious accident”, according to the predicted emissions of ^{137}Cs.

We estimate a number of excess lifetime cancer incidents to be between 20 and 240 for the global population, of which 10–170 may be fatal. These numbers are far lower than the obtained cancer cases after Chernobyl, but somehow comparable to those obtained from the deposition exposure to the Chernobyl-remaining ^{137}Cs over Europe and the total exposure after Fukushima. The last is attributed to the fact that at least 80% of ^{137}Cs from Fukushima was deposited in the oceans, whereas the rest was over populated regions. However, those risks are expected to be higher for the areas around the contaminated forests. This is mainly explained by the existence of a highly radioactive bulk of isotopes that have remained near the plant due to their refractory nature (e.g. isotopes of Pu and ^{241}Am). If they were remobilized they could reach population centers of central Europe affecting the locals.

Concerning living organisms in those forests, even at the worst-case scenario, computerized tools predict weak radiation-related effects. However, evolutionary biologists ring alarm bells for changes in local organism populations of birds and mammals exposed to high radiation since 1986. Nevertheless, the accumulation of radioactivity in certain types of organisms (e.g. fungi) poses an additional, and also indirect, risk for the local human population due to their dietary habits.

Finally, it should be pointed out that the three fire scenarios studied here take into account a conservative approach on the redistribution of ^{137}Cs (only 40% of what is deposited will be emitted) and on its effective half-life (which shows how much ^{137}Cs is still present). However, experiments have shown that these portions strongly depend on the prevailing temperatures during a wildfire (and can reach 100%) and specific ecological properties, respectively. This shows that up to more than 10 PBq of ^{137}Cs may be displaced doubling (or even more) doses and radiation-related cancers over Europe.

Conflict of interest statement

The authors declare that there are no conflicts of interest.

Acknowledgements

This study was funded by the GIS Climat-Environnement-Société (http://www.gisclimat.fr/projet/radioclimfire). It was also granted access to the HPC resources of [CCRT/TGCC/CINES/IDRIS] under the allocation 2012-t2012012201 made by GENCI (Grand Equipement National de Calcul Intensif).

Appendix A. Supplementary data

Supplementary data to this article can be found online at http://dx.doi.org/10.1016/j.envint.2014.08.012.

References

Amiro BD, Sheppard SC, Johnston FL, Evenden WG, Harris DR. Burning radionuclide question: what happens to iodine, cesium and chlorine in biomass fires? Sci Total Environ 1996;187:93–103.

Aoyama M, Hirose K, Suzuki Y, Inoue H, Sugimura Y. High levels of radioactive nuclides in Japan in May. Nature 1986;321:819–20.

Bergan TD. Ecological half-lives of radioactive elements in semi-natural systems. NKS(97) FR5 87-7893-025-1; 2000 [Available: http://www.google.fr/url?sa=t&rct=j&q=&esrc=s&source=web&cd=1&ved=0CCwQFjAA&url=http%3A%2F%2Fwww.nks.org%2Fscripts%2Fgetdocument.php%3Ffile%3D111010111119702&ei=L2fvUtarL6e60QWz1YHQDQ&usg=AFQjCNELZEJfsaT2sG-oC7etpyt-Iy105A&sig2=sW6R3PTBBHTc-Nr1PGzyhQ&bvm=bv.60444564,d.d2k [accessed 5 April 2014]].

Boice Jr JD. Radiation epidemiology: a perspective on Fukushima. J Radiol Prot 2012;932:N33–40.

Brandt J, Christensen JH, Frohn LM. Modelling transport and deposition of caesium and iodine from the Chernobyl accident using the DREAM model. Atmos Chem Phys 2002;2:397–417.

Brown JE, Thørring H, Hosseini A. The "EPIC" impact assessment framework: towards the protection of the Arctic environment from the effects of ionising radiation. In: Barnett CL, Børretzen P, Beresford N, Golikov S, Kryshev I, Oughton DH, Sazykina T, Stensrud H, Wright SM, editors. Deliverable D6 report for EU Funded Project ICA2-CT-2000-10032. Østerås, Norway: Norwegian Radiation Protection Authority; 2003. [Available: https://wiki.ceh.ac.uk/download/attachments/115802239/EPIC_D6.pdf?version=1&modificationDate=1263909651000 [accessed 14 November 2013]].

Bunzl K, Kracke W, Schimmack W. Vertical migration of plutonium-239 + -240, americium-241 and caesium-137 fallout in a forest soil under spruce. Analyst 1992;117(3):469–74.

Christoudias T, Lelieveld J. Modelling the global atmospheric transport and deposition of radionuclides from the Fukushima Dai-ichi nuclear accident. Atmos Chem Phys 2013;13:1425–38.

Cooper JR, Randle K, Sokhi RS, editors. Radioactive releases in the environment: impact and assessment. Wiley 978-0-471-89923-5; 2003. p. 150.

Cuttler JM. Commentary on using LNT for radiation protection and risk assessment. Dose–Response 2010;8:378–83.

Dancause KN, Yevtushok L, Lapchenko S, Shumlyansky I, Shevchenko G, Wertelecki W, et al. Chronic radiation exposure in the Rivne-Polissia region of Ukraine: implications for birth defects. Am J Hum Biol 2010;22. [667–274].

De Cort M, Dubois G, Fridman SD, Germenchuk MG, Izrael YA, Janssens A, et al. Atlas of caesium deposition on Europe after the Chernobyl accident. Luxembourg: Office for Official Publications of the European Communities 92-828-3140-X; 1998 [Catalogue number CG-NA-16-733-29-C. EUR 16733].

ECMWF. ERA-40, forty-year European re-analysis of the global atmosphere. 2002. [Available: http://www.ecmwf.int/products/data/archive/descriptions/e4. [accessed 1 November 2013]].

EPA. Review of ecological assessment case studies from a risk assessment perspective volume II. Washington, DC: United States Environmental Protection Agency, Risk Assessment Forum; 1994 [EPA 630-R-94-003. Available: http://www.epa.gov/raf/publications/pdfs/ECORISK.PDF [accessed 10 February 2013]].

EPA. Cancer risk coefficients for environmental exposure to radionuclides. United States Environmental Protection Agency; 1999 [EPA 402-R-99-001. Available: http://www.epa.gov/radiation/docs/federal/402-r-99-001.pdf [accessed 10 February 2013]].

Evangeliou N, Balkanski Y, Cozic A, Møller AP. Simulations of the transport and deposition of ^{137}Cs over Europe after the Chernobyl NPP accident: influence of varying emission-altitude and model horizontal and vertical resolution. Atmos Chem Phys 2013a;13:7183–98.

Evangeliou N, Balkanski Y, Cozic A, Møller AP. Global transport and deposition of ^{137}Cs following the Fukushima NPP accident in Japan. Emphasis in Europe and Asia using high-resolution model-versions and radiological impact assessment to the population and the environment using interactive tools. Environ Sci Technol 2013b;47:5803–12.

Evangeliou N, Balkanski Y, Cozic A, Møller AP. Global and local health risk assessment after the Fukushima Nuclear Power Plant accident as seen from Chernobyl: a modeling study for radiocaesium (^{134}Cs & ^{137}Cs). Environ Int 2014b;64:17–27.

Evangeliou N, Balkanski Y, Cozic A, Hao WM, Mouillot F, Thonicke K, et al. Fire regime evolution in the radioactively contaminated forests of Ukraine and Belarus: risks foreseen for the European population and the environment from ^{137}Cs displacement. Ecol Monogr 2014w. [accepted].

Feely HW, Helfer IK, Juzdan ZR, Klusek CS, Larsen RJ, Leifer R, et al. Fallout in the New York metropolitan area following the Chernobyl accident. J Environ Radioact 1988;7:177–91.

Fromm MD, Servranckx R. Transport of forest fire smoke above the tropopause by supercell convection. Geophys Res Lett 2003;30(10):1542. http://dx.doi.org/10.1029/2002GL016820.

Fromm M, Torres O, Diner D, Lindsey D, Vant Hull B, Servranckx R, Shettle EP, Li Z. Stratospheric impact of the Chisholm pyrocumulonimbus eruption: 1. Earth-viewing satellite perspective, J Geophys Res 2008;113. http://dx.doi.org/10.1029/2007JD009153.D08202.

Golikov VYu, Balonov MI, Jacob P. External exposure of the population living in areas of Russia contaminated due to the Chernobyl accident. Radiat Environ Biophys 2002;41(10):185–93.

Hatano Y, Hatano N, Amano H, Ueno T, Sukhoruchkin AK, Kazakov SV. Aerosol migration near Chernobyl: longterm data and modeling. Atmos Environ 1998;32:2587–94.

Hoffman FO, Kocher DC, Apostoaei AI. Beyond dose assessment: using risk with full disclosure of uncertainty in public and scientific communication. Health Phys 2012;102:591–2.

Horrill AD, Kennedy VH, Paterson IS, McGowan GM. The effect of heather burning on the transfer of radiocaesium to smoke and the solubility of radiocaesium associated with different types of heather ash. J Environ Radioact 1995;29:1–10.

Hourdin F, Issartel JP. Sub-surface nuclear tests monitoring through the CTBT xenon network. Geophys Res Lett 2000;27:2245–8.

IAEA. Present and future environmental impact of the Chernobyl accident. 1011-4289International Atomic Energy Agency; 2001 [IAEA-TECDOC-1240].

IAEA. INES: The International Nuclear and Radiological Event Scale. Available: http://www-ns.iaea.org/tech-areas/emergency/ines.asp, 2013. [accessed 19 November 2013].

IARC. Estimated cancer incidence, mortality, prevalence and disability-adjusted life years (DALYs) worldwide in 2008: International Agency for Research on Cancer, GLOBOCAN 2008 database, version 3.0. Available: http://globocan.iarc.fr/, 2008. [accessed 16 November 2012].

ICRP. Age-dependent doses to members of the public from intake of radionuclides: International Commission on Radiation Protection, Part 4. ICRP publication. 71Pergamon Press Oxford; 1995.

ICRP. Low-dose extrapolation of radiation-related cancer risk: International Commission on Radiation Protection. Publication 99. Ann. ICRP 35, 4. , 4; 2005 [Available: http://www.icrp.org/publication.asp?id=ICRP%20Publication%2099 [accessed 14 January 2013]].

IPCC. Working Group I: contribution to the IPCC Fifth Assessment Report (AR5), Climate Change. The physical science basis: Intergovernmental Panel on Climate Change, Stockholm: 23–26 September 2013; 2013 [Available: http://www.ipcc.ch/report/ar5/wg1/#.UnkVD5EfWMM [accessed 5 November 2013]].

IRL. Radioecology research of the Red Forest Proving Ground [website]. Kyiv, Ukraine: International Radioecology Laboratory, Chornobyl Center for Nuclear Safety, Radioactive Waste and Radioecology; 2013 [Available: http://www.chornobyl.net/en/index.php?newsid=1174890890 [accessed 23 August 2013]].

Jones S. Windscale and Kyshtym: a double anniversary. J Environ Radioact 2007;99:1–6.

Joshi SR. Early Canadian results on the long-range transport of Chernobyl radioactivity. Sci Total Environ 1987;63:125–37.

Kashparov VA, Lundin SM, Zvarich SI, Yoschenko VI, Levtchuk SE, Khomutinin YuV, et al. Territory contamination with the radionuclides representing the fuel component of Chernobyl fallout. Sci Total Environ 2003;317(1–3):105–19.

Larsson C-M. The FASSET framework for assessment of environmental impact of ionising radiation in European ecosystems — an overview. J Radiol Prot 2004;24:A1–A12.

Larsson C-M. An overview of the ERICA Integrated Approach to the assessment and management of environmental risks from ionising contaminants. J Environ Radioact 2008;99:1364–70.

Lavoué D, Liousse C, Cachier H, Stocks BJ, Goldammer JG. Modeling of carbonaceous particles emitted by boreal and temperate wildfires at northern latitudes. J Geophys Res 2000;105(D22):26871–90.

Little MP, Wakeford R, Janet Tawn E, Bouffler SD. Risks associated with low doses and low dose rates of ionizing radiation: why linearity may be (almost) the best we can do. Radiology 2009;251:6–12.

Lujanieneo G, Plukis A, Kimtys E, Remeikis V, Jankünaiteo D, Ogorodnikov BI. Study of ^{137}Cs, ^{90}Sr, ^{239,240}Pu, ^{238}Pu and ^{241}Am behavior in the Chernobyl soil. J Radioanal Nucl Chem 2002;251:59–68.

Masson O, Baeza A, Bieringer J, Brudecki K, Bucci S, Cappai M, et al. Tracking of airborne radionuclides from the damaged Fukushima Dai-ichi nuclear reactors by European networks. Environ Sci Technol 2011;45:7670–7.

Matsueda M. Predictability of Euro-Russian blocking in summer of 2010. Geophys Res Lett 2011;38. http://dx.doi.org/10.1029/2010GL046557. [L06801].

McMullin S, Giovanetti GK, Green MP, Henning R, Holmes R, Vorren K, et al. Measurement of airborne fission products in Chapel Hill, NC, USA from the Fukushima Dai-ichi reactor accident. J Environ Radioact 2012;112:165–70.

Møller AP, Mousseau TA. Biological consequences of Chernobyl: 20 years after the disaster. Trends Ecol Evol 2006;21:200–7.

Møller AP, Mousseau TA. Reduced abundance of raptors in radioactively contaminated areas near Chernobyl. J Ornithol 2008;150:239–46.

Møller AP, Mousseau TA. Reduced abundance of insects and spiders linked to radiation at Chernobyl 20 years after the accident. Biol Lett 2009;5:356–9.

Møller AP, Mousseau TA. Conservation consequences of Chernobyl and other nuclear accidents. Biol Conserv 2011;114:2787–98.

Møller AP, Mousseau TA. Assessing effects of radiation on abundance of mammals and predator–prey interactions in Chernobyl using tracks in the snow. Ecol Indic 2013;26:112–6.

Mousseau TA, Milinevsky G, Kenney-Hunt J, Møller AP. Highly reduced mass loss rates and increased litter layer in radioactively contaminated areas. Oecologia 2014;175:429–37.

MUEAPPCCC. Atlas: Ukraine: radioactive contamination. , 52Kiev, Ukraine: Ministry of Ukraine of Emergencies and Affairs of Population Protection from the Consequences of Chernobyl Catastrophe; 2008.

NASA. Gridded population of the world: National Aeronautical Space Agency. Available: http://sedac.ciesin.columbia.edu/data/collection/gpw-v3, 2013. [accessed 14 November 2013].

NRC. Health risks from exposure to low levels of ionizing radiation. BEIR VII Phase 2. United States National Research Council; 2006 [Report ISBN: 0-309-09156-5].

NRU. National Report of Ukraine (2011) reports proceedings, conclusions and recommendations. International conference twenty-five years after Chernobyl accident: safety for the future, April 20–22 2011. Ukraine: KIM Kyiv; 2011.

OECD. Health at a glance: Europe 2012. Organisation for Economic Co-operation and Development. OECD Publishing; 2012 [Available: http://dx.doi.org/10.1787/9789264183896-en [accessed 1 March 2014]].

Paatero J, Vira J, Siitari-Kauppi M, Hatakka J, Holmén K, Viisanen Y. Airborne fission products in the high Arctic after the Fukushima nuclear accident. J Environ Radioact 2012;114:41–7.

Paliouris G, Taylorb HW, Wein RW, Svoboda J, Mierzynski B. Fire as an agent in redistributing fallout ^{137}Cs in the Canadian boreal forest. Sci Total Environ 1995; 160/161:153–66.

Paugam R, Wooster M, Papadakis G, Schultz M. Estimation of the injection height of biomass burning emission. Proc. of the ESA-iLEAPS-EGU joint conference; 2010. [Frascati, Italy].

Pentreath RJ, editor. Nuclear power; man and the environment. London, UK: Taylor & Francis LTD; 1980.

Piga D. Residence time of Cs-137 in the atmosphere (PhD Thesis) France: Universite du Sud Toulon Var; 2010 (in French).

Price BN, Jayaraman B. Indoor exposure to radiation in the case of an outdoor release. Lawrence Livermore National Laboratory; 2006. Report LBNL-60662; 2006 Available: http://e-reports-ext.llnl.gov/pdf/335508.pdf [accessed 14 November 2013].

Ritchie JC, McHenry JR. Application of radioactive fallout cesium-137 for measuring soil erosion and sediment accumulation rates and patterns: a review. J Environ Qual 1990;19:215–33.

Shuton VN, Bruk GY, Basalaeva LN, Vasilevitskiy VA, Ivanova NP, Kaplun IS. The role of mushrooms and berries in the formation of internal exposure doses to the population of Russia after the Chernobyl accident. Radiat Prot Dosim 1996;67:55–64.

Sofiev M, Vankevich R, Ermakova T, Hakkarainen J. Global mapping of maximum emission heights and resulting vertical profiles of wildfire emissions. Atmos Chem Phys 2013; 13:7039–52.

Stohl A, Seibert P, Wotawa G, Arnold D, Burkhart JF, Eckhardt S, et al. Xenon-133 and caesium-137 releases into the atmosphere from the Fukushima Dai-ichi nuclear power plant: determination of the source term, atmospheric dispersion, and deposition. Atmos Chem Phys 2012;12:2313–43.

Strode SA, Ott LE, Pawson S, Bowyer TW. Emission and transport of cesium-137 from boreal biomass burning in the summer of 2010. J Geophys Res 2012;117. http://dx.doi.org/10.1029/2011JD017382. (D09302).

Szopa S, Balkanski Y, Cozic A, Deandreis C, Dufresne J-L, Hauglustaine D, et al. Aerosol and Ozone changes as forcing for climate evolution between 1850 and 2100. Clim Dyn 2012. http://dx.doi.org/10.1007/s00382-012-1408-y.

Ten Hoeve JE, Jacobson MZ. Worldwide health effects of the Fukushima Daiichi nuclear accident. Energ Environ Sci 2012;5:8743–57.

Tsushima H, Iwanaga M, Miyazaki Y. Late effect of atomic bomb radiation on myeloid disorders: leukemia and myelodysplastic syndromes. Int J Hematol 2012;95(3): 232–8.

Tubiana M, Feinendegen LE, Yang CC, Kaminski JM. The linear no-threshold relationship is inconsistent with radiation biologic and experimental data. Radiology 2009;251:13–22.

UNPD. Les inégalités d'espérance de vie dans le monde (in French) United Nations Population Division; 2014 [Available: http://inegalites.fr/spip.php?article1423 [accessed 16 June 2014]].

UNSCEAR. Sources, effects and risks of ionizing radiation. Report to the General Assembly, with scientific annexes. New York, NY: United Nations Scientific Committee on the Effects of Atomic Radiation; 1993. [E.94.IX.2, United Nations].

UNSCEAR. Medical radiation exposures. Report to the General Assembly with scientific annexes. Annex ANew York: United Nations Scientific Committee on the Effects of Atomic Radiation; 2008a. [Available: http://www.unscear.org/docs/reports/2008/09-86753_Report_2008_Annex_A.pdf [accessed 25 November 2013]].

UNSCEAR. Exposures of the public and workers from various sources of radiation. Report to the General Assembly with scientific annexes. Annex BNew York: United Nations Scientific Committee on the Effects of Atomic Radiation; 2008b. [Available: http://www.unscear.org/docs/reports/2008/11-80076_Report_2008_Annex_D.pdf [accessed 25 November 2013]].

UNSCEAR. Summary of low-dose radiation effects on health. United Nations Scientific Committee on the Effects of Atomic Radiation; 2010. Report ISBN 978-92-1-642010-9: 2010. Available: http://www.unscear.org/docs/reports/2010/UNSCEAR_2010_Report_M.pdf [accessed 4 November 2013].

Urbanski SP, Salmon JM, Nordgren BL, Hao WM. A MODIS direct broadcast algorithm for mapping wildfire burned area in the western United States. Remote Sens Environ 2009;113:2511–26.

WHO. Preliminary dose estimation from the nuclear accident after the 2011 Great East Japan earthquake and tsunami. World Health Organisation 978 92 4 150366 2; 2012 [Available: http://whqlibdoc.who.int/publications/2012/9789241503662_eng.pdf [accessed 14 November 2013]].

Woodhead DS. Levels of radioactivity in the marine environment and the dose commitment to the marine organisms. , 158/31Vienna: I.A.E.A. – S.M; 1973.

Chernobyl. In: Yablokov AV, Nesterenko VB, Nesterenko AV, editors. Consequences of the catastrophe for people and nature. New York, NY: New York Academy of Sciences; 2009.

Yoschenko VI, Kashparov VA, Protsak VP, Lundin SM, Levchuk SE, Kadygrib AM, et al. Resuspension and redistribution of radionuclides during grassland and forest fires in the Chernobyl exclusion zone: part I. Fire experiments. J Environ Radioact 2006; 86:143–63.

Zibtsev SV, Oliver CD, Goldammer JG, Hohl AM, Borsuk OA. Wildfires management and risk assessment in the Chernobyl Nuclear Power Plant Exclusion Zone. Twenty-five years after Chernobyl accident. Safety for the future — Proceedings of the International Conference. — Kyiv, Ukraine, 20-22 April; 2011. p. 187–91.